Dalton Transactions

Accepted Manuscript

This article can be cited before page numbers have been issued, to do this please use: K. Ypsilantis, T. Tsolis, A. Kourtellaris, M. Manos, J. C. Plakatouras and A. Garoufis, *Dalton Trans.*, 2016, DOI: 10.1039/C6DT04035G.

This is an Accepted Manuscript, which has been through the Royal Society of Chemistry peer review process and has been accepted for publication.

Accepted Manuscripts are published online shortly after acceptance, before technical editing, formatting and proof reading. Using this free service, authors can make their results available to the community, in citable form, before we publish the edited article. We will replace this Accepted Manuscript with the edited and formatted Advance Article as soon as it is available.

You can find more information about Accepted Manuscripts in the author guidelines.

Please note that technical editing may introduce minor changes to the text and/or graphics, which may alter content. The journal's standard Terms & Conditions and the ethical guidelines, outlined in our author and reviewer resource centre, still apply. In no event shall the Royal Society of Chemistry be held responsible for any errors or omissions in this Accepted Manuscript or any consequences arising from the use of any information it contains.

ROYAL SOCIETY OF CHEMISTRY

rsc.li/dalton

View Article Online
DOI: 10.1039/C6DT04035G

SYNTHESIS, REACTIVITY AND CHARACTERIZATION OF Pt(II) COMPLEXES WITH N,N' CHELATING LIGANDS; STRUCTURE AND DIMETHYLSULFOXIDE REACTIVITY RELATIONSHIP.

Konstantinos Ypsilantis,[a] Theodoros Tsolis,[a] Andreas Kourtellaris,[b] Manolis J. Manos,[a] John C. Plakatouras[a] and Achilleas Garoufis[a].*

[a]Department of Chemistry, University of Ioannina, GR-45110 Ioannina, Greece

[b]Department of Chemistry, University of Cyprus, P.O. Box 20537, CY-1678 Nicosia, Cyprus

ABSTRACT

Platinum(II) complexes of the formula $PtLCl_2$ [L= 2-(2'-pyridyl)quinoxaline, (pqx) (**1**) 2,(2'-pyridyl)benzo[*g*]quinoxaline, (pbqx) (**3**) and 2,(2'-pyridyl)quinoline, (pqn) (**5**)] were synthesized and characterized by spectroscopic and x-ray diffraction methods. Also, monodentate coordination of the ligands pqx and pbqx formed the complexes *trans*-Pt(DMSO)pqxCl_2 (**2**) and *trans*-Pt(DMSO)pbqxCl_2 (**4**) as it is indicated from x-ray crystal structure and NMR studies. The reaction of the complexes (**1**), (**3**) and (**5**) with DMSO-d_6 revealed a ligand-release solvolysis, which was studied by means of NMR techniques. Correlation between the crystal structures of (**1**), (**3**), (**5**) and kinetic or thermodynamic parameters of the solvolysis reactions showed that the tendency of the ligands pqx, pbqx, and pqn to return in the *anti-* configuration in addition to the ability of non-classical H-bonds, are crucial factors for the ligand-release solvolysis. Instantaneous DMSO-d_6 solvolysis for the complexes (**1**) and (**3**) and slow kinetics solvolysis for (**5**) ($k = 10^{-4} \pm 6.4 \times 10^{-6}$ s^{-1}) reflect their structural differences in ligand planarity. Based on NMR techniques a two-step mechanism of the chelate ring opening was suggested with equilibrium constants of the overall reaction at 298 K, $K_{eq} = 4.1 \pm 0.2 \times 10^{-4}$ M^{-1} (**1**) and $K_{eq} = 1.7 \pm 0.2 \times 10^{-4}$ M^{-1} (**2**).

Keywords: anticancer drugs, square planar Pt(II) complexes,

* Corresponding author

View Article Online
DOI: 10.1039/C6DT04035G

Introduction

Platinum chemotherapeutic compounds are among the most potent drugs in cancer chemotherapy [1]. Cisplatin, carboplatin and oxaliplatin bind coordinatively to DNA bases, causing DNA bending and cell apoptosis [2]. Side effects and the limitation of an effective dose due to the drugs toxicity draw the research interest in other types of platinum compounds as potential anticancer drugs. Nowadays, two main classes of Pt(II) compounds with different action mechanism from cisplatin are under intense investigation; dinuclear [3-7] or polynuclear complexes [8, 9], and platinum metallointercalators [10-14]. The latter are, in general, cationic complexes with a saturated platinum coordination sphere with four nitrogen donor atoms, which usually come from aromatic diimines. Such compounds bind non-coordinatively to DNA through their aromatic ligands, causing significant alterations to the DNA helix [15, 16]. Despite the stability of these complexes, offered by the 5-membered chelate ring(s), in some cases the complexes decompose in solvents such as DMSO [10].

On the other hand DMSO is a commonly used solvent, dissolving non-water soluble metal complexes in order to study their biological activity [17]. In some cases the complexes solvolyse in DMSO, and usually the chloro ligands are replaced, due to the high affinity of platinum to coordinate with sulfur containing ligands [18]. Thus, the DMSO solvolysis of complexes with the general formula $PtCl_2L$ (L is ethylenediamine [19] or various N-methylated ethylenediamines [20]) mainly leads to the replacement of the chloro ligand by DMSO.

However, the dissociation of an NN' chelate aromatic diimine from platinum center by DMSO is reported very rarely. Two decades ago it had been reported that complexes of the formula $PtLCl_2$ (L = 2,2'-bipyridyl-3,3'-dicarboxylic acid or 3,3'-dimethylol-2,2'-bipyridine) release the chelate ligand L, after dissolution in DMSO-d_6 [21]. More recently, J. Aldrich-Wright et al reported that the complex $[Pt(pqx)(dach)]Cl_2$ (pqx= 2,(2'-pyridyl) quinoxaline and dach = *1R,2R*- or *1S,2S*-diaminocyclohexane) decomposes in DMSO [10]. In both cases the studied complexes deviate from the square planar geometry, while most significant is the deviation of the planarity of the aromatic ligand.

In an attempt to clarify the above query and with the ambition to correlate the complex structure with its reactivity with DMSO, complexes of the formula $PtLCl_2$ [L= 2,(2'-pyridyl) quinoxaline, (pqx) 2,(2'-pyridyl)benzo[*g*]quinoxaline, (pbqx) and 2,(2'-pyridyl)quinoline, (pqn)] were synthesized and characterized, both in solution and solid state. Their reactivity with DMSO-d_6 was studied by means of NMR spectroscopic techniques. Also, the different binding modes of the above ligands were discussed.

View Article Online
DOI: 10.1039/C6DT04035G

Experimental

Materials and methods

All solvents were of analytical grade and were used without further purification. Potassium tetrachloroplatinate(II) (99.9%) was purchased from Alfa Aesar. 2,(2'-pyridyl)quinoxaline [22], 2,(2'-pyridyl)benzo[*g*]quinoxaline [23] and 2,(2'-pyridyl)quinoline [24] were prepared as previously described. The complex *cis*-$PtCl_2(DMSO)_2$ was prepared according to the literature methods [25].

C, H, N determinations were performed on a Perkin-Elmer 2400 Series II analyzer. Absorption spectra were measured in a Jasco V-650 spectrophotometer in a 1 cm path length cuvette for the region 900-220 nm. ^{1}H NMR spectra were recorded on a Bruker Avance spectrometer operating at ^{1}H frequencies of 500.13 MHz or 400.13 MHz and processed using Topspin 3.1 (Bruker Analytik GmbH). ^{195}Pt NMR spectra were recorded operating at frequency 85.99 MHz. ^{195}Pt chemical shifts were referenced relative to external standard $K_2[PtCl_4]$ in D_2O (δ ^{195}Pt = -1630 ppm) [26]. Two-dimensional COSY and TOCSY experiments assisted the proton signal assignments.

Solvolysis of complex (5) in DMSO-d_6.

The solvolysis of the complex (**5**) in DMSO-d_6 was monitored by ^{1}H NMR spectroscopy in DMSO-d_6 at concentration of 10 mM at 298 K. The solvolysis reaction follows slow kinetic in the NMR time scale at 298 K and the fraction (F) of the solvolysis products was calculated from the ratio (r_i) of relative integrals, between selected proton signals of the initial complex and the final reaction product, according to equation (1). Then, the F was converted to concentration units (M), based on the initial concentration of 10 mM.

$$F = r_i/(1+r_i) \qquad (1)$$

Plot of concentration of the reaction product *vs.* time was fitted with pseudo-first order kinetics equation (2) to give the rate constant *k*.

$$A = A_1 - A_2\, e^{-kt} \qquad (2)$$

A_1 and A_2 are constants related to the initial and equilibrium concentration of (**5**).

X-Ray crystallography

Suitable single crystals covered with paratone-N oil were attached on the tip of glass fibers. X-ray diffraction data were collected (ω-scans) with a Oxford Diffraction Xcalibur-3 diffractometer under a flow of nitrogen gas at 100(2) K using Mo Kα radiation (λ = 0.71069 Å). Data were collected and processed by using the CRYSALIS CCD and RED software [27] respectively. Empirical

View Article Online
DOI: 10.1039/C6DT04035G

absorption corrections (multiscan based on symmetry related measurements) were applied using CrysAlis RED software. The structures were solved by direct methods using SIR2014 [28] and refined on F^2 using full-matrix least-squares with the latest version of SHELXL [29]. All non-H atoms were refined anisotropically and carbon-bound H-atoms were introduced at calculated positions and allowed to ride on their parent atoms. The refinement of the structures was not without problems and special details can be found in the deposited CIF files in addition to full structural details. Geometric/crystallographic calculations were carried out using PLATON, [30] and WINGX [31] packages; graphics were prepared with X-Seed [32]. The CCDC files 1510648 - 1510651 contain the supplementary crystallographic data for this paper. This data can be obtained free of charge from the Cambridge Crystallographic Data Centre via ccdc.cam.ac.uk/products/csd/request.

Synthesis of the complexes

Pt(pqx)Cl_2 (1): Although the synthesis of the Pt(pqx)Cl_2 has been published very recently [10], here a different method is presented. An amount of 20 mg (0.05 mmol) of *cis*-PtCl_2(DMSO)$_2$ was dissolved in 10 mL of hot chloroform and a solution containing 10 mg (0.05 mmol) of pqx in 3 mL of chloroform was added. The mixture was left to react for 24h at 50 °C in the dark without stirring. During the reaction time a crystalline orange precipitate appeared which was collected with filtration, washed with chloroform (2 × 5 mL) and dried under vacuum over P_2O_5. Some crystals were of suitable size for X-ray diffraction measurements. Yield 93%. $C_{13}H_9Cl_2N_3Pt$: calc.% C, 33.00; H, 1.92; N, 8.88. Found C, 32.90; H, 2.01; N, 8.86. ^{1}H NMR ($CDCl_3$, 298 K, δ in ppm, 500 MHz), H3 9.44 (s, 1H); H5 8.27 (d, 1H); H6 7.98 (t, 1H); H7 8.05 (m, 1H); H8 9.87 (d, 1H); H3’ 8.28 (d, 1H); H4’ 8.29 (t, 1H); H5’ 7.75 (t, 1H); H6’ 10.00 (d, 1H).

***trans*-Pt(pqx)(DMSO)Cl_2 (2)**: An amount of 20 mg (0.05 mmol) of *cis*-PtCl_2(DMSO)$_2$ was dissolved in 50 mL of chloroform. After cooling the solution to about 10 °C, a solution containing 10 mg (0.05 mmol) of pqx in 3 mL of chloroform was added. The mixture was left to react for 24h in the dark at 10 °C. Slow diffusion of Et_2O in the reaction mixture formed a crystalline light orange precipitate which was collected with filtration, washed with cold chloroform (1 × 1 mL), diethyl ether (2 × 5 mL) and dried under vacuum over P_2O_5. Some of the crystals were suitable for X-ray measurements. Yield 75%. $C_{15}H_{15}Cl_2N_3OPtS$: calc. (%) C, 32.72; H, 2.86; N, 7.58. Found C, 32.60; H, 2.71; N, 7.58. ^{1}H NMR ($CDCl_3$, 298 K, δ in ppm, 500 MHz), H3 10.18 (s, 1H); H5 8.81 (d, 1H); H6 7.48 (t, 1H); H7 7.97 (m, 1H); H8 8.61 (d, 1H); H3’ 8.24 (d, 1H); H4’ 7.97 (t, 1H); H5’ 7.99 (t, 1H); H6’ 9.31

View Article Online
DOI: 10.1039/C6DT04035G

(d, 1H); DMSO-CH_3 3.57 (s, 6H). ^{195}Pt NMR ($CDCl_3$, 298 K, ppm, 85.99 MHz), -3040 ppm. A few crystals, suitable for X-ray diffraction analysis, were collected from the microcrystalline solid.

Pt(pbqx)Cl_2 (3): An amount of 20 mg (0.05 mmol) of *cis*-$PtCl_2(DMSO)_2$ was dissolved in 10 mL of hot chloroform and a solution containing 12 mg (0.05 mmol) of pbqx in 5 mL of chloroform was added. The mixture was left to react for 24h at 50 °C in the dark without stirring. During the cooling of the reaction mixture a crystalline red precipitate appeared which was collected with filtration washed with chloroform (2 × 5 mL) and dried under vacuum over P_2O_5. Slow cooling of the reaction mixture leads to crystals suitable for crystallographic characterization. Yield 90%. $C_{17}H_{11}Cl_2N_3Pt$: calc.% C, 39.02; H, 2.12; N, 8.03. Found C, 39.90; H, 2.31; N, 7.96. ^{1}H NMR ($CDCl_3$, 298 K, δ in ppm, 500 MHz), H3 9.40 (s, 1H); H5 8.86 (s, 1H); H6 8.17 (d, 1H); H7 7.71 (m, 1H); H8 7.78 (m, 1H); H9 8.29 (s, 1H); H10 10.55 (s, 1H); H3’ 8.34 (d, 1H); H4’ 8.33 (t, 1H); H5’ 7.78 (t, 1H); H6’ 10.07 (d, 1H).

Pt(pbqx)(DMSO)Cl_2 (4): An amount of 20 mg (0.05 mmol) of *cis*-$PtCl_2(DMSO)_2$ was dissolved in 50 mL of chloroform. After cooling the solution to about 10 °C, a solution containing 12 mg (0.05 mmol) of pbqx in 5 mL of chloroform was added. The mixture was left to react for 24h in the dark at 10 °C. Slow diffusion of Et_2O in the reaction mixture formed a crystalline red precipitate which was collected with filtration, washed with cold chloroform (1 × 1 mL), diethyl ether (2 × 5 mL) and dried under vacuum over P_2O_5. Yield 80%. $C_{19}H_{17}Cl_2N_3OPtS$: calc. (%) C, 37.94; H, 2.85; N, 6.99. Found C, 37.68; H, 2.91; N, 76.92. ^{1}H NMR ($CDCl_3$, 298 K, δ in ppm, 500 MHz), H3 10.30 (s, 1H); H5 9.86 (s, 1H); H6 8.20 (d, 1H); H7 7.74 (m, 1H); H8 7.75 (m, 1H); H9 8.36 (s, 1H); H10 8.39 (s, 1H); H3’ 8.71 (d, 1H); H4’ 7.99 (t, 1H); H5’ 7.52 (t, 1H); H6’ 8.86 (d, 1H) ; DMSO-CH_3 3.62 (s, 6H). ^{195}Pt NMR ($CDCl_3$, 298 K, ppm, 85.99 MHz), -3038 ppm. A few crystals, suitable for X-ray diffraction analysis, were collected from the crystalline solid.

Pt(pqn)Cl_2 (5): An amount of 20 mg (0.05 mmol) of *cis*-$PtCl_2(DMSO)_2$ was dissolved in 10 mL of hot methanol and a solution containing 10 mg (0.05 mmol) of pqn in 5 mL of methanol was added. The mixture left to react for 24h at 50 °C in the dark without stirring. During the cooling of the reaction mixture a crystalline red precipitate was appeared which was collected with filtration washed with methanol (2 × 5 mL) and dried under vacuum over P_2O_5. Some of the crystals were suitable for X-ray measurements. Yield 90%. $C_{14}H_{10}Cl_2N_2Pt$: calc.% C, 35.61; H, 2.13; N, 5.93. Found C, 35.92; H, 2.21; N, 5.86. ^{1}H NMR (DMSO-d_6, 298 K, δ in ppm, 500 MHz), H3 9.05 (d, 1H); H4 8.62 (d, 1H) H5 8.21 (d, 1H); H6 7.82 (t, 1H); H7 7.96 (t, 1H); H8 9.34 (d, 1H); H3’ 8.75 (d, 1H); H4’ 8.49 (t, 1H); H5’ 7.89 (t, 1H); H6’ 9.50 (d, 1H).

View Article Online
DOI: 10.1039/C6DT04035G

Results and discussion

Solution characterization of the complexes

Schematic demonstration of the structures of the prepared complexes (**1**)-(**5**), with atoms numbering is presented in the following scheme.

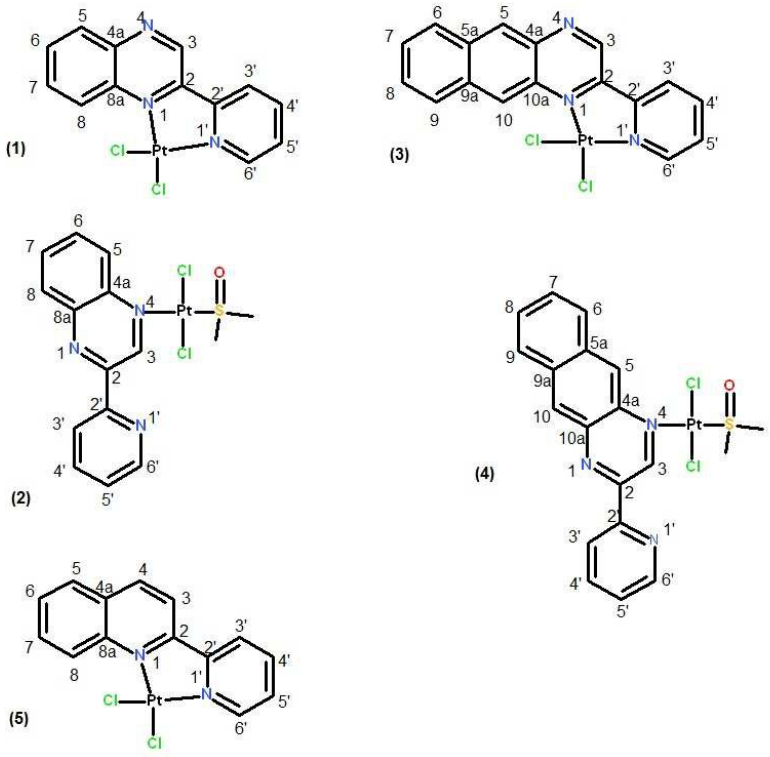

The ^{1}H NMR spectrum of complex (**1**) in $CDCl_3$, (Fig. 1a) shows significant downfield shifts for the protons H6' ($\Delta\delta$ = + 1.23 ppm) and H8 ($\Delta\delta$ = + 1.72 ppm), while the other proton signals of the pqx shifted significantly less. More particularly, the deshielding effect of platinum on the H8 is remarkably large [33], indicating a possible alteration in the configuration of pqx. In addition, the equivalence of H5 and H8 in the free ligand has been lifted, indicating that N1 participates to the coordination sphere. Satellite signals in either side of the H6' doublet, were observed, reflecting the ^{3}J spin–spin interactions with ^{195}Pt nucleus (34%-abundant). The value of $^{3}J_{Pt\text{-}H6'}$ found equals to 38.4 Hz, which is characteristic for vicinal Pt-H6 coupling of pyridine derivatives [34, 35]. The long range coupling constant, $^{4}J_{Pt\text{-}H3}$ = 10.8 Hz, was also observed and it is within the accepted values (10-16 Hz) [34, 35]. All the above observations confirm a N1N1' chelate coordination of pqx.

Similarly, the ^{1}H NMR spectrum of complex (**2**) in $CDCl_3$, (Fig. 1b), shows significant downfield shift for the neighboring to N4 protons, H3 ($\Delta\delta$ = + 0.29 ppm) and H5 ($\Delta\delta$ = + 1.23 ppm), while the proton signals of H6' ($\Delta\delta$ = + 0.09 ppm) and H8 ($\Delta\delta$ = + 0.17 ppm), shifted marginally. Since H6' and H8 are adjacent to N1' and N1, any possibility for coordination through

View Article Online
DOI: 10.1039/C6DT04035G

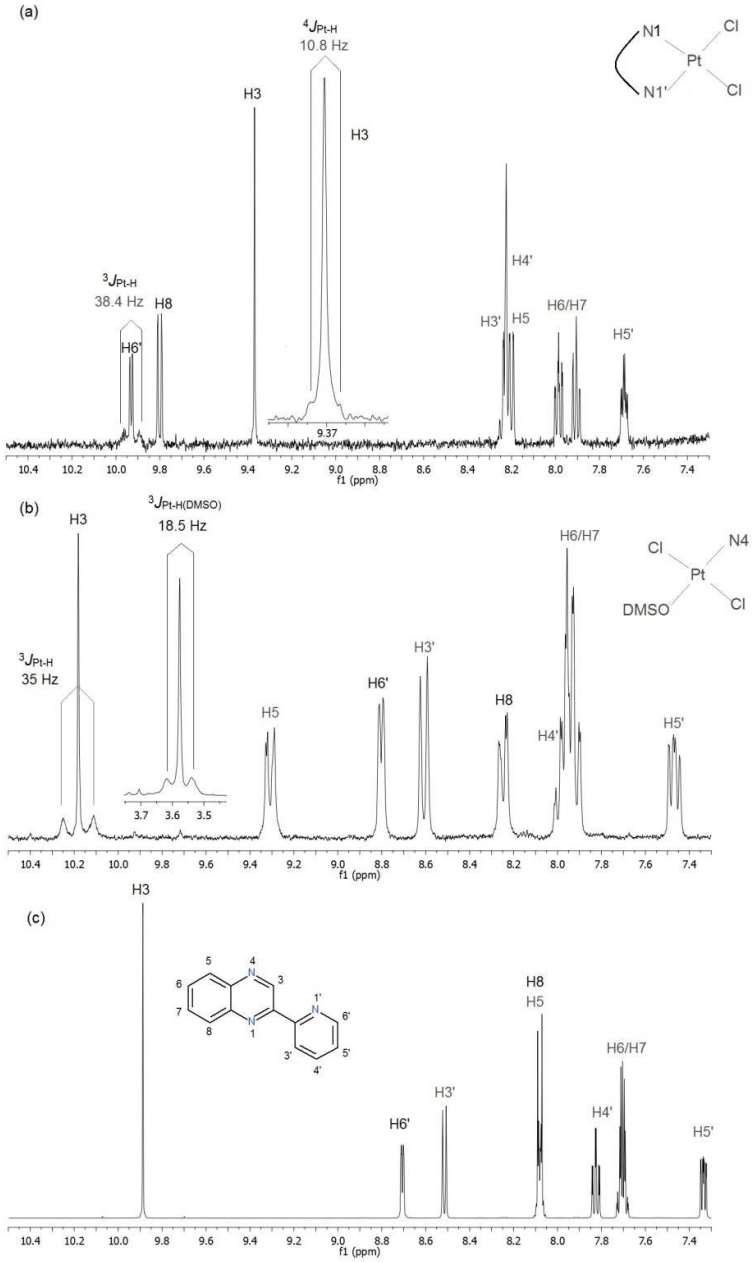

FIGURE 1. (a) Aromatic region of ^{1}H NMR spectrum of (**1**) in $CDCl_3$ @400 MHz at 298K with proton assignments. Inset, a magnification of H3 signal with the rarely observed (only in singets) long-range $^4J_{Pt-H3}$ satellites was presented. (b) Aromatic region of ^{1}H NMR spectrum of (**2**) in $CDCl_3$ @250 MHz at 298K with proton assignments. The ^{195}Pt satellites in H3 are more intense than (**1**) due to the lower resonance field. Inset, the resonance of DMSO methyl groups observed at 3.57 ppm. (c) Aromatic region of ^{1}H NMR spectrum of free pqx in $CDCl_3$ @400 MHz at 298K with proton assignments.

View Article Online
DOI: 10.1039/C6DT04035G

these nitrogen donors atoms is excluded. Furthermore, the satellite-signals in both sides of H3 ($^3J_{Pt-H3}$ = 35 Hz) and the absence of similar signals in H6', indicates a monodentate coordination of pqx only through N4. At higher fields (δ = 3.57 ppm) a singlet, with relative integral corresponding to 6H, was assigned to the coordinated DMSO methyl groups (Δδ = + 1.06 ppm). This singlet is followed by two satellite broad signals giving a $^3J_{Pt-CH3}$ = 18.5 Hz, which is characteristic for coordinated DMSO through sulfur atom [36].

In general substitution reactions of Pt(II) square planar complexes proceed with retention of the configuration [37]. However, the reaction of *cis*-$Pt(DMSO)_2Cl_2$ with pqx results to the complex *trans*-$Pt(DMSO)(pqx)Cl_2$ without retention of the *cis*- configuration [36]. An alternative explanation includes the formation of the anionic complex $[Pt(DMSO)Cl_3]^-$ and a subsequent substitution of the *trans*- to DMSO chloro ligand [38]. However, no NMR evidence of the formation of $[Pt(DMSO)Cl_3]^-$ in $CDCl_3$ was observed. Recently, it has been reported that the value of ΔG_{298} of the reaction *cis*-$Pt(DMSO)LCl_2$ ↔ *trans* -$Pt(DMSO)LCl_2$ (L = (*E*)-*N,N'*-bis(2-pyridyl)iminoisoindoline) is -5 kcal mol^{-1}. This is in agreement with predomination of the *trans*- isomer [39] in the equilibrium. Also, the possibility of a similar isomerization reaction of complex (**2**) cannot be excluded.

However, the different binding mode of the ligand pqx in complexes (**1**) and (**2**) is an issue of even greater interest. So far, many reports indicate that 2-(2'-pyridyl)quinoxaline acts as a chelate ligand through N1 and N1' with various metal ions [40]. Complex (**2**) is the first example where pqx coordinates monodentately through N4, even though in the case of complex $[Hg(CH_2COCH_3)(pqx)]_2$, pqx forms a Hg-N1' strong bond (2.175 Å) and a Hg-N1 very weak (2.560 Å) bond in a bidentate highly asymmetric (anisobidentate) mode [41].

In the cases of (**1**) and (**2**) both complexes have been prepared in the same solvent ($CHCl_3$), with the same starting materials and in the same molar ratios of the reactants. However, the reaction temperature and the time differ. At low temperature (≈ 15 °C) the monodentate (N4) complex (**2**) was formed and at higher temperature (≈ 50 °C) the bidentate (N1N1') was precipitated. This observation can be explained considering the configurations of pqx, *syn* and *anti* (Fig.2). The crystal structure of pqx shows that the preferable configuration in the solid state is the *anti* [42]. In this configuration both H3 and H3' form weak hydrogen bonds with N1' and N1 correspondingly, increasing the deshielding effect on their nuclei. Therefore, their ^{1}H NMR signals should be expected downfield.

View Article Online
DOI: 10.1039/C6DT04035G

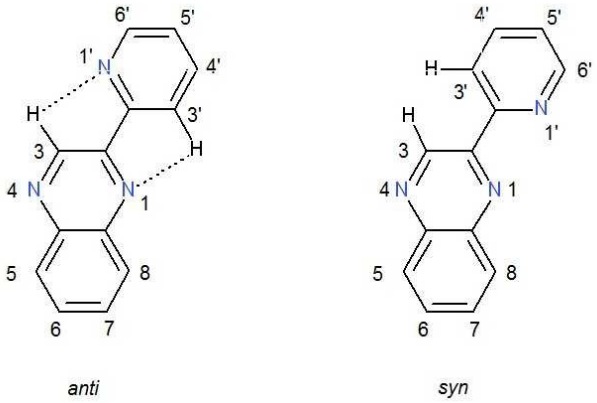

FIGURE 2. *Syn* and *anti* configuration of ligand pqx with atom numbering. Dash lines in the *anti*-conformer show the hydrogen bonds between N1-H3' and N1'-H3.

Indeed, in the ^{1}H NMR spectrum of pqx in $CDCl_3$, the signals of H3' (δ = 8.51 ppm) and H3 (δ = 9.89 ppm) were observed significantly downfield, compared to the other aromatic protons of pqx. Additionally, the absence of ROE signal between the H3 and H3' in the ROESY spectrum of pqx at various t_m, confirms that pqx, most likely, prefers the *anti* configuration in $CDCl_3$ as well as in the solid state. With this in mind it would be easy to understand why complex (**2**) is formed at low temperature and it remains stable at 7 °C in $CDCl_3$ for several days.

On the other hand, at increasing the temperature to 50 °C in a sample of free pqx, no ^{1}H NMR evidence of changes in its conformation was observed. The chemical shifts of the indicator protons H3 and H3' almost remain unchanged, suggesting that pqx tends to adopt the *anti* conformation. However, the reaction with *cis*-$Pt(DMSO)_2Cl_2$ at 50 °C leads to the formation of complex (**1**) where ligand pqx acts bidentately and is forced to adopt the *syn* conformation. In addition, at increasing the temperature of a sample of (**2**) in $CDCl_3$, the complex (**1**) precipitates almost quantitatively. It is reminded that in complex (**2**) the chloro ligands are in *trans*-configuration, while in the resulted (**1**), the chloro ligands are in *cis*. This observation can be explained assuming an intermolecular mechanism as presented in Fig. 3.

The first step of the proposed mechanism includes an intermolecular interaction of the coordinated pqx N1, with platinum, the formation of a five-coordinated intermediate and the secession of the DMSO from the metal coordination sphere. This results in the destruction of N1-H3' weak hydrogen bond and the weakness of the pqx *anti* configuration. Thus, the N1' of pyridinic moiety of pqx interacts with platinum, forming again a five-coordinated intermediate. In

View Article Online
DOI: 10.1039/C6DT04035G

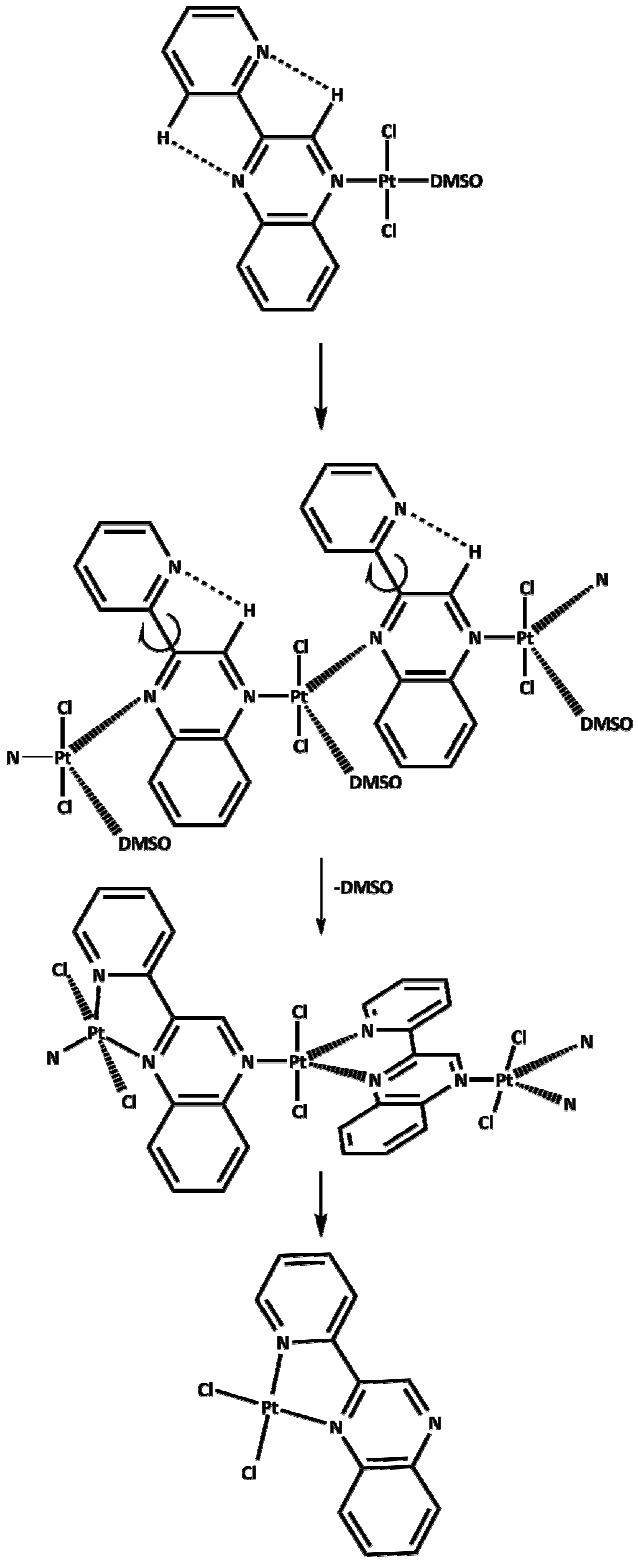

FIGURE 3. Proposed mechanism for transformation of complex (**2**) to (**1**)

this second step the Pt-N4 bond is cleaved due to the higher stability of the five-membered chelate ring, forming the complex (**1**).

View Article Online
DOI: 10.1039/C6DT04035G

In complex (**1**) the ligand pqx adopts the *syn* conformation, the ^{1}H NMR signals of H3 and H3' shifted strongly upfield by -0.55 ppm (δ = 9.44 ppm) and -0.23 ppm (δ = 8.28 ppm) respectively, reflecting the sum of a small downfield shift, due to Pt(II) coordination to N1 and N1', and the upfield shift, due to the abolition of the *anti* conformation. In general, the chemical shift of H3 could be a good indicator of the conformation or the coordination mode of pqx. In an acidified solution of $CDCl_3$, the ^{1}H NMR spectrum of (**1**) shows the singlet of H3 at δ = 9.70 ppm, indicating that N4 of pqx is protonated. Thus, it could be concluded that the deshielding effect on H3 nucleus increases with the order: pqxN4-platination (δ = 10.18 ppm) > pqx *anti* configuration (δ = 9.89 ppm) > N1N1'-platination and N4-protonation (δ = 9.70 ppm) > N1N1'-platination (δ = 9.44 ppm). In other words, the interaction between H3 and N1' in pqx *anti* conformer, is strong enough to deshield significantly the H3.

The ^{1}H NMR spectra of complexes (**3**) and (**4**) in $CDCl_3$ show enough similarities with these of (**1**) and (**2**). The spectrum of (**3**) shows significant downfield shifts for the protons H6' and H10, which are neighboring to the coordination sites N1' and N1. The H6' shifted by 1.27 ppm (δ = 10.07 ppm) and the H10 by 1.80 ppm (δ = 10.55 ppm). The rest protons of pyridine moiety, shifted downfield (H4' and H5'), with the exception of H3', which shifted upfield by 0.33 ppm.

The above observations, together with two satellite peaks on both sides of H6' signal ($^{3}J_{Pt\text{-}H6'}$ = 39.2 Hz), clearly indicate that pbqx coordinates to Pt(II) through N1'and N1. A noteworthy upfield shift of the proton H3 ($\Delta\delta$ = 0.87 ppm) reflects again the alteration of the pbqx configuration from *anti* to *syn*. This value is higher than the corresponding upfield shift ($\Delta\delta$ = 0.64 ppm) of H3 in complex (**1**), probably due to the higher electron withdrawal from H3 as a result of the additional aromatic ring of pbqx.

The ^{1}H NMR spectrum of (**4**) in $CDCl_3$ shows a downfield shift of H3 (-0.23 ppm) and H5 (-1.10 ppm). The signals of H6' and H10 which are close to N1' and N1 respectively shifted marginally by 0.03 and 0.10 ppm, excluding any possibility of coordination through these nitrogen atoms. Furthermore the observation of $^{3}J_{Pt\text{-}H3}$ = 36 Hz confirms the monodentate coordination of pbqx. A singlet peak at δ = 3.62 ppm ($^{3}J_{Pt\text{-}CH3}$ = 20 Hz) with relative integral ratio to pbqx 6:1, indicates that only one molecule of DMSO is included in the platinum coordination sphere. The absence of crystallographic data does not allow the determination of complex (**4**) configuration with assurance. However, the similarities of chemical shifts in ^{1}H NMR signal of the coordinated DMSO methyl groups and the ^{195}Pt NMR (δ = -3037 ppm), indicate that most probably (**4**) is in the same *trans*- configuration as complex (**2**).

View Article Online
DOI: 10.1039/C6DT04035G

Complex (**5**) is insoluble in $CDCl_3$ and the ^1H NMR spectra of a freshly prepared sample of (**5**), as well as the free ligand, were recorded in MeOD-d_4. The ^1H NMR of (**5**) shows a significant downfield shift for the H6' ($\Delta\delta$ = 0.73 ppm) while the other protons of the pyridinic moiety of pqn, shifted downfield in a range of 0.1 - 0.5 ppm. It is worth mentioning that the H3' shifted downfield by 0.12 ppm, in contrast to upfield shifts that were observed in the cases of complexes (**1**) ($\Delta\delta$ = 0.23 ppm) and (**3**) ($\Delta\delta$ = 0.33 ppm). In addition, a downfield shift was observed for H3 ($\Delta\delta$ = 0.52 ppm) in contrast to upfield shifts observed in the cases of H3 in (**1**) ($\Delta\delta$ = 0.55 ppm) and (**3**) ($\Delta\delta$ = 0.87 ppm). These observations lead to the conclusion that the *anti* conformer in the case of free pqn is less preferable than that of pqx and pbqx. A possible explanation may be derived from the differences in δ^+ charge of H3 that is less in the case of pqn than that of pqx, due to the less electronegative C4 than the N4. Less δ^+ charge means weaker hydrogen bonding with N1' and therefore less preferable the *anti* conformation. The downfield shift of pqn H8 ($\Delta\delta$ = 1.29 ppm), that is relatively lower than those observed in the similar complexes (**1**) ($\Delta\delta$ = 1.72 ppm) and (**3**) ($\Delta\delta$ = 1.80 ppm), confirms the N1N1' coordination of pqn.

Crystal structures of (1), (2), (3) and (5)

Crystals of complexes (**1) – (3)** and (**5)** (Fig. 4) suitable for X-ray structure determination were obtained from the parent solutions. Selected bond lengths and angles are presented in Table 1. As shown in Fig. 4, all of them have distorted square planar coordination about platinum. Complex (**2)** is the *trans* isomer with monodentate coordination of the nitrogen ligand opposite to DMSO's sulfur atom, while the rest are *cis*, as imposed by the heterocycle chelate. Those structural data provide us the opportunity to compare the effect of the multi-ring system to the geometry of the coordination sphere and the overall complex. Detailed structural information can be found in the supplementary material.

View Article Online
DOI: 10.1039/C6DT04035G

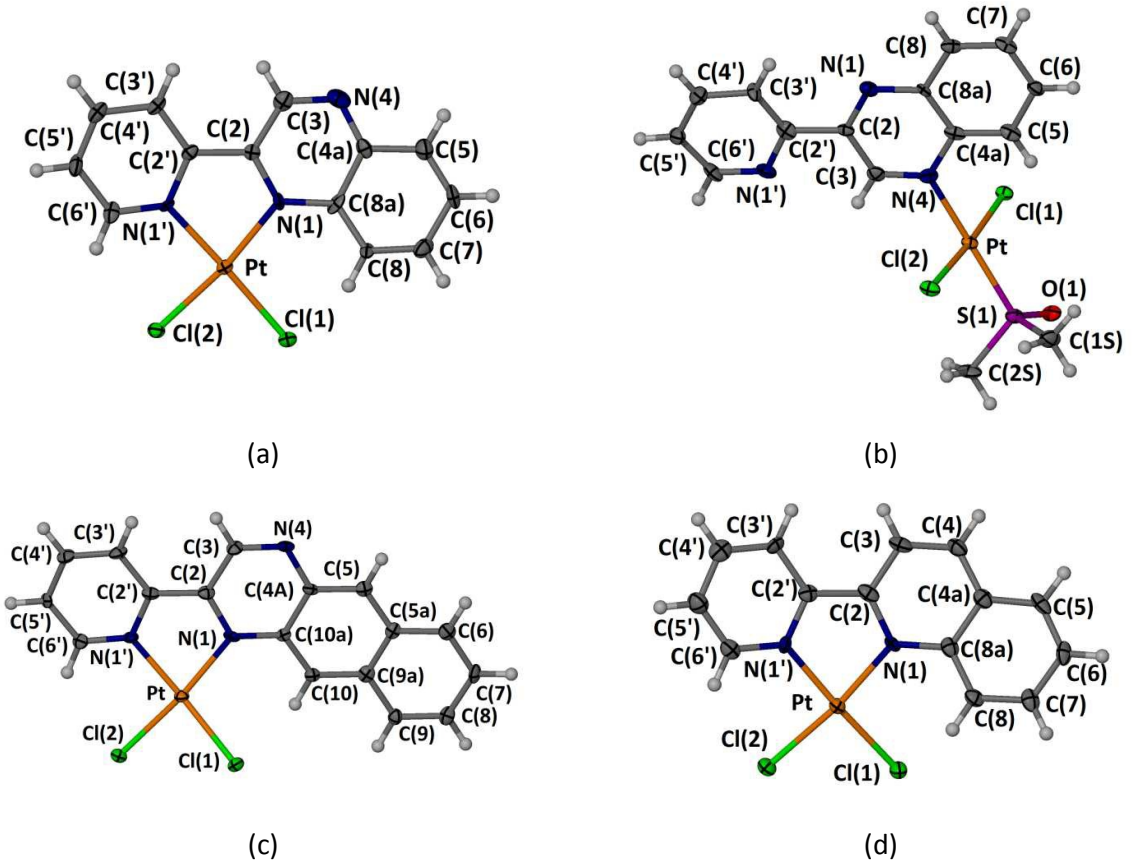

FIGURE 4. Thermal ellipsoid presentations (50 % probability level) of the molecular structures of compounds: a) [Pt(pqx)Cl_2], (**1**), b) *trans*-[Pt(pqx)(DMSO)Cl_2], (**2**), c) [Pt(pbqx)Cl_2], (**3**), d) [Pt(pqn)Cl_2], (**5**).

The Pt – N bond distances span the range 2.003 to 2.079 Å, while the Pt – Cl lengths are in the range 2.293 - 2.318 Å, and are in agreement with literature data [22, 43, 44]. The same appears with the Pt – S bond distance which is 2.214 Å, and fits literature data (two examples are given in [45]). The differences in the Pt – N bond distances, though small, appear to be systematic.

The entire Pt – $N_{pyridine}$ bonds are shorter than the adjacent Pt – N bonds, in complexes (**1**), (**3**) and (**5**), indicating the increased nucleophilicity of the pyridine nitrogen atom. When the Pt – N bond distances of the different complexes are compared, it seems that in deciding the differences, π-back bonding is more important than σ-bonding. This way, the Pt – N bond distances in (**3**) are shorter than the corresponding in (**1**) with consistency to the more extended LUMO orbital of pbqx related to the same orbital of pqx (mean Pt – N for (**1**) and (**3**) are 2.054 and 2.036 Å, respectively). When (**5**) is included in the discussion, it becomes obvious that the replacement of the nitrogen atom of the quinoxaline heterocyclic ring (position 4 in Fig.4) with the less

View Article Online
DOI: 10.1039/C6DT04035G

electronegative carbon, leads to increased negative charge on nitrogen and even stronger σ-bonding, and shorter Pt – N bond distances (mean Pt – N for (**5)** is 2.025 Å).

TABLE 1. Coordination sphere bond distances (Å) and angles (°) of the structurally characterized complexes.

[Pt(pqx)Cl_2] **(1)**			
Pt – Cl(1)	2.318(5)	Pt – Cl(2)	2.294(4)
Pt – N(1)	2.079(13)	Pt – N(1')	2.029(17)
Cl(1) – Pt – Cl(2)	85.20(16)	Cl(1) – Pt – N(1)	102.0(5)
Cl(1) – Pt – N(1')	176.7(4)	Cl(2) – Pt – N(1)	172.1(5)
Cl(2) – Pt – N(1')	92.2(4)	N(1) – Pt – N(1')	80.5(6)
trans-[Pt(pqx)(DMSO)Cl_2] **(2)**			
Pt – Cl(1)	2.314(3)	Pt – Cl(2)	2.303(3)
Pt – S(1)	2.214(2)	Pt – N(4)	2.053(8)
Cl(1) – Pt – Cl(2)	176.23(11)	Cl(1) – Pt – S(1)	93.16(9)
Cl(1) – Pt – N(4)	90.1(2)	Cl(2) – Pt – S(1)	90.07(10)
Cl(2) – Pt – N(4)	86.7(2)	S(1) – Pt – N(4)	176.1(2)
[Pt(pbqx)Cl_2] **(3)**			
Pt – Cl(1)	2.306(3)	Pt – Cl(2)	2.293(2)
Pt – N(1)	2.054(8)	Pt – N(1')	2.019(7)
Cl(1) – Pt – Cl(2)	86.86(9)	Cl(1) – Pt – N(1)	99.8(2)
Cl(1) – Pt – N(1')	169.5(2)	Cl(2) – Pt – N(1)	173.2(2)
Cl(2) – Pt – N(1')	92.8(2)	N(1) – Pt – N(1')	80.8(3)
[Pt(pqn)Cl_2] **(5)**			
Pt – Cl(1)	2.302(2)	Pt – Cl(2)	2.297(2)
Pt – N(1)	2.046(7)	Pt – N(1')	2.003(8)
Cl(1) – Pt – Cl(2)	88.10(7)	Cl(1) – Pt – N(1)	98.7(2)
Cl(1) – Pt – N(1')	171.55(18)	Cl(2) – Pt – N(1)	172.7(2)
Cl(2) – Pt – N(1')	93.3(2)	N(1) – Pt – N(1')	79.6(3)

The differences in the Pt – Cl bond distances are of the same or slightly smaller magnitude as in the Pt – N distances, and they reflect the greater *trans* influence of the pyridine ring than the part of the ligands that contain fused aromatic rings [46]. For example, in complex (**1)**, the Pt – Cl(1) bond distance, which is *trans* to the Pt – $N_{pyridine}$ bond, is longer than the Pt – Cl(2) bond distance, which is *trans* to the Pt – $N_{quinoxaline}$ bond. This rationalization can be applied successfully to complexes (**3)** and (**5)**, as well.

The distortions from the ideal square planar geometry can easily be realized comparing the coordination sphere angles, with complex (**2)** been the less distorted. This is expected since all ligands are monodentate, and the bite angle of the nitrogen chelate is absent. Those distortions

View Article Online
DOI: 10.1039/C6DT04035G

can also be seen from the deviations of the least square planes calculated for the coordination sphere of the complexes. Thus, compound (**3)**, being the most distorted, has N(1') 0.14 Å out of the Pt(donor)$_4$ least squares plane; in (**5)** the deviation is 0.08 for N(1'), while in complexes (**1)** and (**2)**, which are the less distorted from that point of view, Pt and Cl(1) deviate 0.04 Å, respectively.

As mentioned in the synthetic part, (**1)** has been synthesized previously [10]**.** Aldrich-Wright's compound has slightly different coordination sphere characteristics (it complies with the above discussion) and it is crystallized in a different unit cell (monoclinic *vs* hexagonal). Those differences indicate the dependence of the structural characteristics on the crystal form and the sensitivity of the coordination sphere to the weak packing interactions. The major difference of the two structures is that the published complex forms dimmers through metallophilic interactions (Pt – Pt, 3.832 Å), whilst our product has stronger interactions, forming 1D chains parallel to *c* axis (Pt – Pt, 3.472 Å). The existence of those two polymorphs resembles the red and yellow polymorphs of Pt(bpy)Cl$_2$. The red polymorph displays columnar Pt – Pt interactions [47] whilst the yellow polymorph displays aromatic ring stacking without Pt – Pt interactions [48]. This explains the color difference in the later pair of polymorphs; the former pair has no significant color differences due to metallophilic interactions in both polymorphs.

Solvolysis of (1), (3) and (5) in DMSO-d$_6$

Structure and ligand releasing relationships

The dissolution of (**1**) and (**3**) in DMSO-d$_6$ leads to the complete and instantaneous release of the ligands pqx and pbqx from the platinum center, resulting to the complex Pt(DMSO-d$_6$)$_2$Cl$_2$ and the free ligands, as evidenced from ^{1}H and ^{195}Pt NMR spectroscopy. Thus, in the ^{1}H NMR spectra of (**1**) and (**3**), in DMSO-d$_6$, only one set of signals was observed, corresponding to the free ligands. Also, the ^{195}Pt NMR spectra of the same samples show a signal at δ = -3442 ppm matching the value of Pt(DMSO-d$_6$)$_2$Cl$_2$ (δ = -3443 ppm). Similarly, complex (**5**) reacts with DMSO-d$_6$, releasing the ligand pqn and producing Pt(DMSO-d$_6$)$_2$Cl$_2$ but in a significantly slower rate than (**1**) and (**3**) (Fig. S1). This difference allowed the monitoring of the reaction by ^{1}H NMR spectroscopy. During the time, the intensities of the ^{1}H NMR signals of the complex (**5**) decrease and new signals pop up until the solvolysis reaction was completed, indicating a slow kinetics in the NMR time scale at 298 K ($k < 10^{-1}$ s^{-1}). The new signals were matching exactly to the free pqn in DMSO-d$_6$. A plot of the free pqn concentration vs. time, based on relative integrals of selected signals, fitted with the pseudo-first order kinetics equation (**2**) gives a rate constant $k_{obs} = 10^{-4} \pm 6.4 \times 10^{-6}$ s^{-1} (Fig. 5). It is well known that substitution reactions in Pt(II) complexes follow a two-term rate law: [49, 50]

View Article Online
DOI: 10.1039/C6DT04035G

$$\text{rate} = k_1[\text{complex}] + k_2[\text{complex}]\,[\text{nucleophilic}] \qquad (3)$$

Under pseudo-first order kinetics equation (3) is simplified to (4):

$$\text{rate} = k\,[\text{complex}] \qquad (k = k_1 + k_2\,[\text{nucleophilic}]) \qquad (4)$$

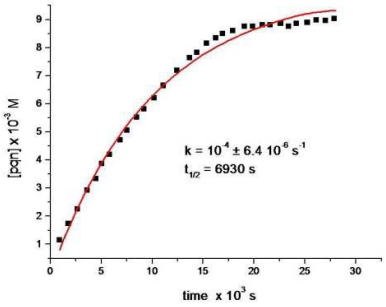

FIGURE 5. Plot of changes in pqn concentration (10^{-3} M) vs. time (s) during the solvolysis of (**5**) at 298 K, fitted by the first order equation $A = A_1 - A_2\, e^{-kt}$, using the software Origin v. 5 (Microcal software Ltd).

So far, it is easy to conclude that the solvolysis of (**1**) and (**3**) is not related to the N4 of pqx and pbqx, since complex (**5**), which has no such nitrogen atom, solvolysed as well. In addition, from the first point of view, the differences in the Pt – N bond lengths do not justify the differences in the stability of the complexes, especially if we take into account well known stable complexes with similar bond distances. For example, platinum complexes with 3,3' substituted bpy, have shorter Pt-N bond distances than (**1)**, (**3)** and (**5)**, and comparable distances with bpy and bpm complexes, but decompose in DMSO; $Pt(bpy)Cl_2$ and $Pt(bpm)Cl_2$ (bpy = 2,2'-bipyridine and bpm = 2,2'-bipyrimidine), resisted to the ligand release in DMSO-d_6 at 298K for several weeks.

It is easy to say that the common denominator in all these three complexes (**1**), (**3**) and (**5**) is the bulky shape of the ligand, which causes a significant deviation from the square planar geometry (as shown in the description of the structures), but the exact factors which affect the stability remain unclear. The thorough study of the structural characteristics of the prepared complexes in comparison with other complexes is essential to shed some light on the factors that govern this behavior.

Hazell [51] has developed and applied geometric criteria to account for the distortions of bpy in metal complexes, while Marzilli et al [43] have applied those, successfully, in a series of Pt and Pd complexes. To assess the distortions and correlate them with the stability of our complexes we can use two of the above mentioned criteria (θ_{di}, the dihedral angle between the two best least squares planes calculated for the ligand's ring systems, and θ_s, the dihedral angle between

View Article Online
DOI: 10.1039/C6DT04035G

the two best planes calculated for the donor atoms of the coordination sphere and the four atoms, NCC'N of the chelated part of the ligand). Additionally, we can use the torsion angle (T) formed by the NCC'N', which readily proves a distorted planar ligand and the two dihedral angles (θ_1 and θ_2) formed by the ligand rings and the plane formed by the donor atoms. The last two angles are indicative of how symmetrical is the distortion of the chelated ligand relative to the planar coordination sphere. These distortions in the prepared complexes are depicted in Fig. 6. Table 2 summarizes crystallographic data of the distortion parameters of pqx, pbqx and pqn, together with parameters from crystal structures of similar complexes retrieved from the Cambridge Structural Database (CSD) [52] .

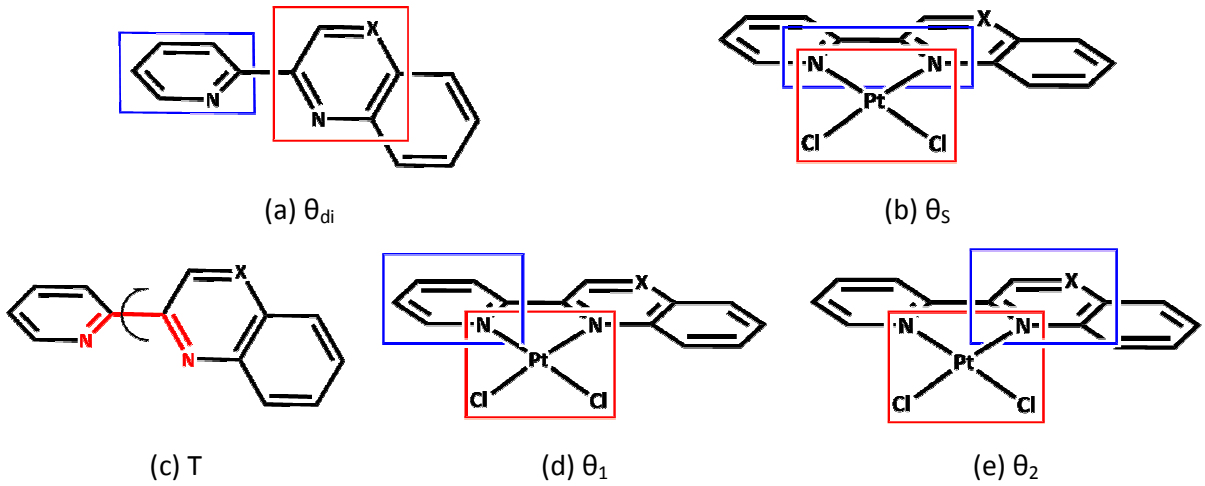

FIGURE 6. The structural criteria used to assess the distortions of the prepared complexes.

The purpose of the first two groups of compounds included in Table 2 is to show that the geometrical characteristics of the pseudo square planar complexes of Pt(II) are dependent on the solid state; those differences can be considered minor. In the first group are the two polymorphs of $Pt(bpy)Cl_2$, mentioned previously, and a complex which is co-crystallized with a salt formulated as $[(tppz)Pt_2(bpy)_2](BF_4)_4$ (where tppz = tetra-(2-pyridine)pyrazine); $Pt(bpy)Cl_2$ is stacked between the bpy moieties of the dinuclear cation [53]. The second group contains $Pt(bpm)Cl_2$, (bpm = 2,2'-bipyrimidine) and two solvated compounds. Again, there are small structural differences and distortions, which can be neglected from the discussion.

The third group contains six Pt(II) complexes, all of them with substituted bipyridines. A comparison of their characteristics can be rather enlightening. Complexes $Pt(4,4'\text{-}Me_2bpy)Cl_2$ and $Pt(5,5'\text{-}Me_2bpy)Cl_2$ present negligible distortions and are stable in DMSO, while the other four

View Article Online
DOI: 10.1039/C6DT04035G

TABLE 2. Distortion parameters of (**1**), (**3**) and (**5**) and similar complexes.

Compound[a]	Pt-N[b]	θ_{di}	θ_S	T	θ_1	θ_2	CSD code	Ref.
$Pt(bpy)Cl_2$ (red)		0.0	0.0	0.0	0.0	0.0	BPYCPT03	47
$Pt(bpy)Cl_2$ (yellow)	2.006[c]	4.1	3.6	0.7	3.7	5.3	BPYCPT10	48
$Pt(bpy)Cl_2$		6.9	3.3	5.1	3.9	8.4	RIGLIE	53
$Pt(bpm)Cl_2$		7.8	5.7	1.8	5.9	6.6	XOZWUE	54
$Pt(bpm)Cl_2$·DMF	2.004[c]	2.4	1.8	0.4	1.6	2.6	NOYXOO	55
$Pt(bpm)Cl_2$·NMP		4.4	3.0	0.0	3.4	3.4	RINNOR	56
$Pt(4,4'\text{-}Me_2bpy)Cl_2$	2.025	2.8	5.0	2.3	5.5	7.3	TIHVEM	43
$Pt(5,5'\text{-}Me_2bpy)Cl_2$	2.017	5.4	0.9	3.7	3.0	3.0	PERDIZ02	43
$Pt(6,6'\text{-}Me_2bpy)Cl_2$	2.026	20.3	36.8	5.2	39.0	35.5	TIHVIQ	43
$Pt(3,3'\text{-}(HOOC)_2bpy)Cl_2$	2.009	26.2	8.8	22.7	15.0	20.1	NEKYAD	22
$Pt(3,3'\text{-}(MeOOC)_2bpy)Cl_2$	1.991	25.5	8.9	21.3	14.5	19.2	PERDOF	44
$Pt(3,3'\text{-}(HOCH_2)_2bpy)Cl_2$	2.017	28.9	11.4	22.3	16.0	23.7	NEKYEH	22
$Pt(pqx)Cl_2$ (**1**)	2.033[c]	11.8	12.4	7.2	10.7	17.5		
$Pt(pqx)Cl_2$		17.1	24.3	3.5	21.5	27.6	SUQLIB	10
$Pt(pbqx)Cl_2$ (**3**)	2.039	9.1	20.3	5.4	19.5	21.3		
$Pt(pqn)Cl_2$ (**5**)	2.026	17.8	24.9	6.7	21.0	30.1		
$Pt(bqu)Cl_2$	2.031	17.6	35.7	4.3	37.9	34.7	GAWQOL	57

[a] See text for the abbreviations of the ligands; [b] mean values; [c] mean value for all compounds.

complexes are significantly distorted, and they decompose in DMSO. Compounds $Pt(3,3'\text{-}(HOOC)_2bpy)Cl_2$, $Pt(3,3'\text{-}(MeOOC)_2bpy)Cl_2$, and $Pt(3,3'\text{-}(HOCH_2)_2bpy)Cl_2$ show important differences on the parameters presented in Table 2, related to the former groups, but their distortions are very similar among the subgroup. The reason for those distortions in the complexes of the 3,3'-disubstituted bipyridines and their subsequent decomposition is probably the tendency of the ligands to return to the *anti*- conformation due to steric hindrance of the bulky substitutes in 3 and 3' sites. There are two opposite forces that affect the planarity of this family of ligands. The first one is the repulsive force between the substituents on the 3 and 3' positions of the chelate, which tends to rotate the two rings in such a way so the 3 and 3' substituents have the longest possible distance; the other is the coordination to the transition metal, which is directional and forces the NCC'N' system to be as planar as possible. The combination of those two leads to the bowing distortion as described by Hazell [51]. As an example, to prove this assumption, we can take the case of 3,3'-dimethyl-2,2'-bipyridine; unfortunately there are no Pt(II) or Pd(II) complexes

View Article Online
DOI: 10.1039/C6DT04035G

in the literature but there are quite a few complexes with other metals in CSD [52]. When 3,3'-Me_2bpy is bonded to a transition metal, the NCC'N' torsion T, though it is big enough due to the steric effect of the methyl groups, it is smaller than the same torsion T in rare earth complexes, where the covalent character of the M – N bond is reduced and eventually the directionality of the coordination to the metal ion.

Comparing the structural parameters of Pt(6,6'-Me_2bpy)Cl_2 with the other members of the group we see that the θ_S angle is the biggest, while θ_1 and θ_2 are close to each other with the torsion angle T comparable to the stable complexes. 6,6'-Me_2bpy's plane is folded relative to coordination plane, and this is due to the strain induced by the repulsion between the methyl group and the chloro ligand. Similar structural behavior can be found in the pair Pt(phen)Cl_2 [58] and Pt(2,9-Me_2phen)Cl_2 [59].

The forth group includes complexes with ligands containing fused aromatic rings. The compounds (**1)**, (**3)**, and (**5)**, synthesized in this work, the polymorph of (**1)** and a platinum(II) complex with 2,2'-biquinoline. Obviously the distortions present in the compounds are different from the other groups and when comparing the distortion parameters of this group with the former groups, some important observations can be made.

The θ_{di} angles are smaller than the corresponding in the complexes of 3,3' – substituted bpy's and 6,6' – Me_2bpy, but are significantly larger than those in the complexes of the unsubstituted bpy and 4,4'- a nd 5,5'- substituted bpy's. Note, that there are no substitutions in positions 3,3' and 6,6' to affect the torsion angle T or induce repulsion to the chloro ligands, respectively. The variation of the θ_s angle follows a different pattern from θ_{di}. θ_s is bigger than the corresponding in all other complexes except the 6,6'-Me_2bpy compound.

There are two intramolecular non-conventional H-bonding interactions, Cl ⋯ H – C, formed by the chloro ligands and the hydrogen atom on the 6 and 6' positions of the pyridine rings in all of the above mentioned complexes except in Pt(6,6'-Me_2bpy)Cl_2 (Fig. 7a). Additionally, in the cases where an adjacent fused aromatic ring is present this H-bond is impossible; a different H-bonding interaction is present (Fig. 7b), which, due to the size of the formed ring, leads to increased θ_2 angle, and occasionally in asymmetry between θ_1 and θ_2. The dimensions of those non-conventional H-bonds are presented in Table 3. This way, the distortion and the subsequent instability of the compounds is caused by an attractive force (instead of repulsive as in the case of 6,6'-Me_2bpy) that needs to be accommodated in a six membered ring instead of a five membered. The torsion T is small as mentioned above.

View Article Online
DOI: 10.1039/C6DT04035G

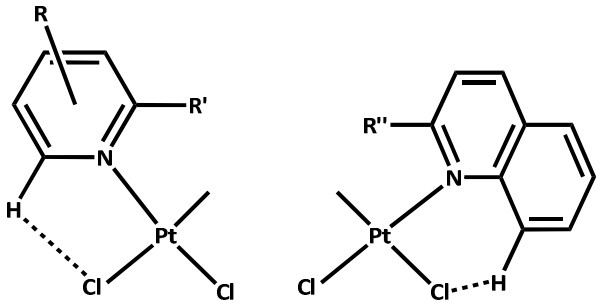

(a) (b)

FIGURE 7. Schematic representation of the non – conventional H-bonds formed in the N,N' bis aromatic chelate platinum(II) complexes. The 5- (a) and 6-membered (b) rings are shown.

TABLE 3. Structural characteristics of the non – conventional H – bonds in (**1**), (**3**) and (**5**) and similar complexes (distances in Å, angles in ^{o}).

Compound	**Type**[1]	**C – H**	**H ··· Cl**	**C ··· Cl**	**C – H ··· Cl**	**CSD code**	**Ref**
$Pt(bpy)Cl_2$ (red)	a[2]	0.95	2.63	3.23	122.1	BPYCPT03	47
$Pt(bpm)Cl_2$	a[2]	0.93	2.74	3.29	119.4	XOZWUE	54
$Pt(4,4'\text{-}Me_2bpy)Cl_2$	a[2]	0.95	2.66	3.26	121.6	TIHVEM	43
$Pt(5,5'\text{-}Me_2bpy)Cl_2$	a[2]	0.95	2.63	3.24	122.3	PERDIZ02	43
$Pt(3,3'\text{-}(HOOC)_2bpy)Cl_2$	a[2]	0.90	2.64	3.22	124.0	NEKYAD	22
$Pt(3,3'\text{-}(MeOOC)_2bpy)Cl_2$	a[2]			3.19[3]		PERDOF	44
$Pt(3,3'\text{-}(HOCH_2)_2bpy)Cl_2$	a[2]	0.93	2.64	3.24	122.0	NEKYEH	22
$Pt(pqx)Cl_2$ (**1**)	a	0.93	2.57	3.15(2)	121		
	b	0.93	2.45	3.17(2)	135		
$Pt(pqx)Cl_2$[3]	a	0.95	2.66	3.20	116.5	SUQLIB	10
	b	0.95	2.49	3.11	123.7		
$Pt(pbqx)Cl_2$ (**3**)	a	0.95	2.56	3.15(2)	121		
	b	0.95	2.44	3.14(2)	131		
$Pt(pqn)Cl_2$ (**5**)	a	0.93	2.69	3.21(1)	117		
	b	0.93	2.26	3.17(1)	121		
$Pt(bqu)Cl_2$	b[2]	0.93	2.64	3.14	115.4	GAWQOL	57

[1] Refers to Figure 7; [2] Mean values; [3] Hydrogen atoms parameters are not given.

From the above discussion it seems that the structural distortion that reduces the stability of these pseudo-square planar Pt(II) complexes is the angle θ_s, which is dependent on three

View Article Online
DOI: 10.1039/C6DT04035G

distinct ligand features: the presence of substituents in (i) 3 and 3', (ii) 6 and 6' positions, and (iii) the size of the ring formed by the C – H ··· Cl interactions.

Titration of the complexes with DMSO-d_6 in $CDCl_3$ solution

The decomposition of complex (**1**) in DMSO-d_6 was further investigated, monitoring the changes of its ^{1}H NMR spectrum in $CDCl_3$, caused by the addition of small portions of DMSO-d_6 (Fig. S2). During the titration two different effects take place. Initially the ^{1}H NMR signals of the complex shifted until the ratio [DMSO-d_6]:[(**1**)] increased about to 1050:1 (fast exchange) and then new signals pop up until the final ratio reaches the value, [DMSO-d_6]:[(**1**)] = 2500:1 (slow exchange). The new signals were exactly matched to the free pqx in an identical mixture of DMSO-d_6:$CDCl_3$ 1:2(v/v), as it is the resultant solvent mixture of the titration.

During the first step of the titration the signals of H8 and H6' shifted upfield by 0.27 and 0.22 ppm, respectively. This observation reflects an almost equal electron density withdrawal from the bonds Pt-N1 and Pt-N1' and will be interpreted as the formation of both complexes (I) and (II), which are presented in Fig. 8C. According to this suggested mechanism, the opening of the chelate ring was achieved from the cleavage of the one Pt-N bond (Pt-N1 or Pt-N1'), followed by the coordination of a DMSO-d_6. Also, the signals of H3 and H3' shifted downfield by 0.46 ppm and 0.40 ppm respectively, towards their values in free pqx in *anti* configuration. The other proton signals shifted slightly in a range of ± 0.05 ppm. Clearly, in this step the DMSO-d_6 does not cause the complete release of pqx from (**1**), but causes the cleavage of the Pt-N1 or Pt-N1' bond. This step is in fast kinetics at the NMR time scale and 298 K, resulting in a rate constant $k_1 > 10^5$ s^{-1} [60]. By adding further portions of DMSO-d_6 and until the ratio increases to the final 2500:1, the pqx proton signals shifted slightly by ± 0.05 ppm, either due to diversification of solvents ($CDCl_3$:DMSO-d_6) ratio or due to the equilibrium of (**1**) with the forms (I) and (II) and the final products of the reaction second step.

Above the ratio 1050:1, the complex begins to release the pqx and it is transformed to the final *cis*-Pt(DMSO-d_6)$_2$Cl$_2$ as also indicated from the ^{195}Pt NMR spectrum (δ ^{195}Pt = -3443 ppm) of the reaction products. This second step takes place in slow kinetics at the NMR time scale and 298 K ($k_2 < 10^{-1}$ s^{-1}). The observed differences in the proton chemical shifts between forms (I) and (II) and the free ligand, are in accordance with the reaction mechanism presented in Fig. 8C. Thus, H6' and H8 signals shift upfield by 0.95 and 1.52 ppm respectively, indicating that pqx is completely

View Article Online
DOI: 10.1039/C6DT04035G

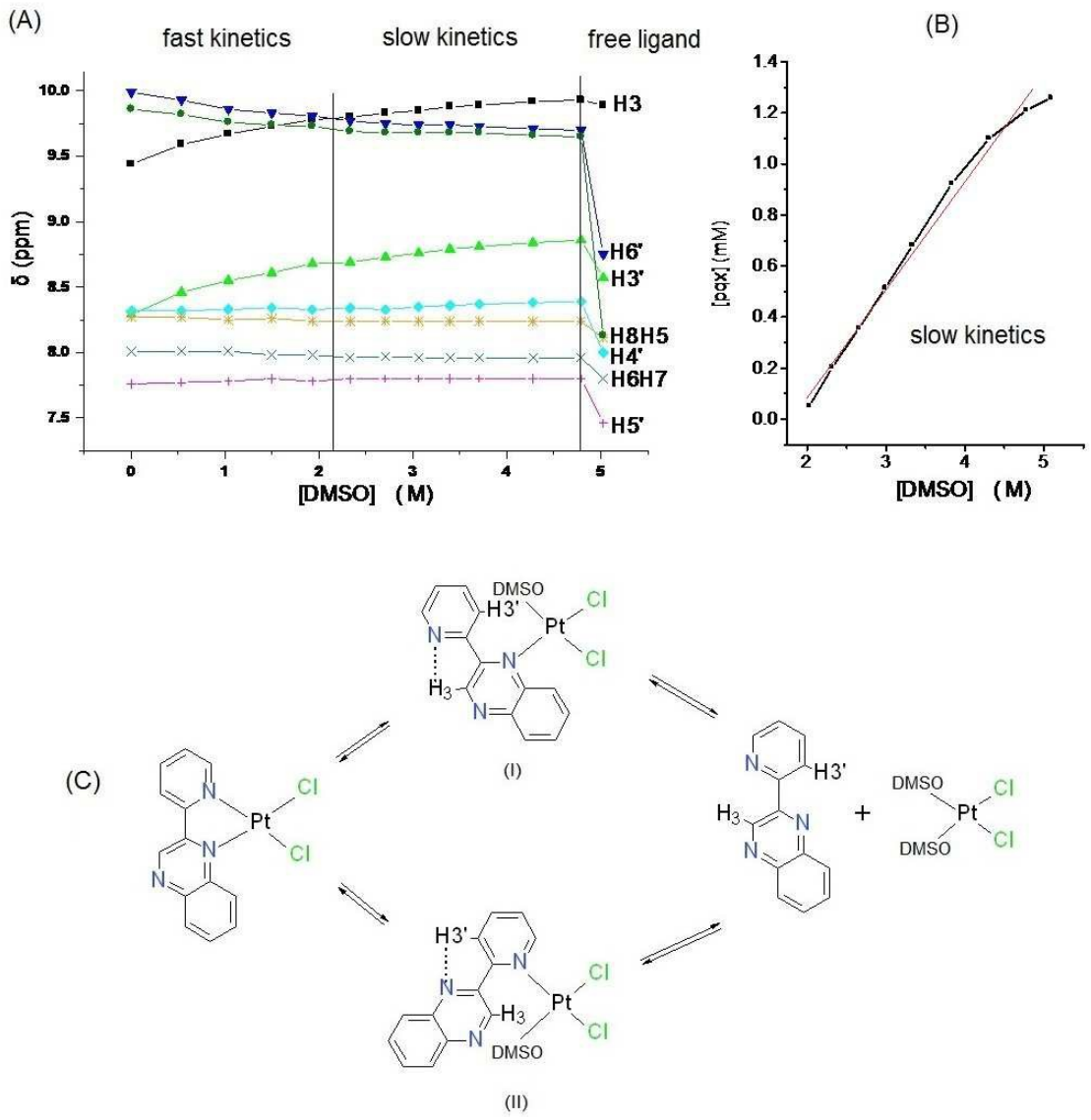

FIGURE 8. (A) Plot of ^{1}H NMR chemical shifts of (**1**) vs. [DMSO-d_6], of a 2 mM solution of (**1**) in $CDCl_3$ titrated with DMSO-d_6. In the plot are noted the [DMSO-d_6] corresponding to fast and slow reaction kinetics at 298 K. Also, the ^{1}H chemical shifts of the free ligand in the reaction solution corresponding to the [DMSO-d_6] 5.03 M are plotted. (B) Plot of free [pqx] vs. [DMSO-d_6], produced from the relative integrals of the arising proton signals and the signals of complex (**1**), during the titration. (C) Suggested mechanism for the reaction of (**1**) with DMSO-d_6.

released from Pt(II). These Δδ values are significantly higher than those observed in the first reaction step (H6' = 0.27 and H8 = 0.22 ppm), indicating a small contribution of this step in the overall reaction. Since the Δ*δ* of H8 is higher to that of H6', it is concluded that the bond Pt-N1 is

View Article Online
DOI: 10.1039/C6DT04035G

mainly cleaved in the second step. Also, the $\Delta\delta$ value of H3 is significantly small (0.04 ppm), indicating that the pyridine ring of pqx is oriented in *anti* configuration from the very first reaction step, that applies only when the bond Pt-N1' is cleaved. Linear fitting of the plot in Fig. 8B results an equilibrium constant of the overall reaction, $K_{eq} = 4.1 \pm 0.2 \times 10^{-4}$ M^{-1}.

Similar behavior was observed for complex (**3**) during the titration of a 1 mM solution of (**3**) in $CDCl_3$ with DMSO-d_6 (Fig. 9). Initially, the ^{1}H NMR signals of (**3**) shifted until the ratio [DMSO-d_6]:[(**3**)] reached the ratio 1750:1 (fast exchange) and then new signals pop-up until the ratio reaches the value, of 3000:1 (slow exchange) (Fig. S3). The new signals were exactly matched to the free pbqx proton signals in an identical mixture of DMSO-d_6:$CDCl_3$ (v/v) 1:1, as it is the resultant solvent mixture of the titration. The equilibrium constants were estimated in a similar manner of (**1**) and calculated as $K_{eq} = 1.7 \pm 0.2 \times 10^{-4}$ M^{-1}. This value is slightly lower from that of complex (**1**), and unfortunately the insolubility of complex (**5**) in $CDCl_3$ or in other non-coordinative solvents, did not allow a similar titration with DMSO-d_6.

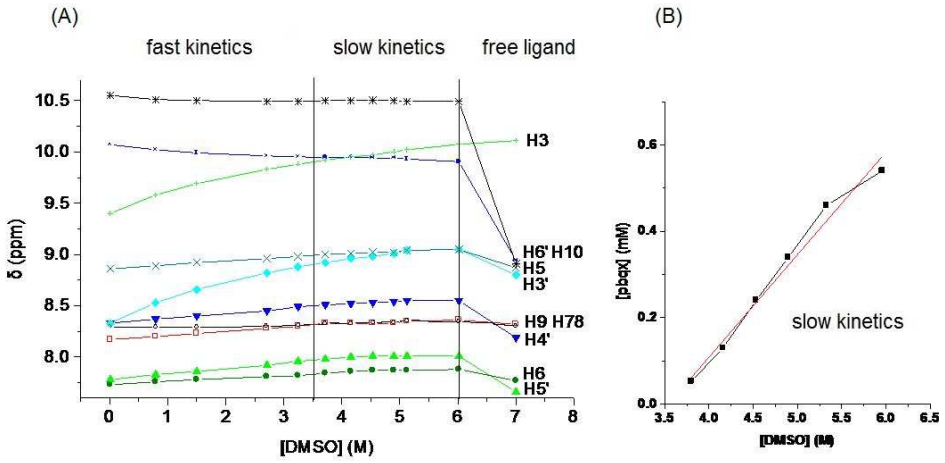

FIGURE 9. (A) Plot of ^{1}H NMR chemical shifts of (**5**) vs. [DMSO], of a 1 mM solution in $CDCl_3$, titrated with DMSO-d_6. In the plot are noted the [DMSO-d_6] corresponding to fast and slow reaction kinetics at 298 K. Also, the ^{1}H chemical shifts of the free ligand in the reaction solution corresponding to the [DMSO-d_6] 7.0 M are plotted. (B) Plot of free [pbqx] vs. [DMSO-d_6], produced from the relative integrals of the arising proton signals and the signals of complex (**1**), during the titration.

View Article Online
DOI: 10.1039/C6DT04035G

Certainly, the correlation of structural characteristics in the solid state with solution reactivity is a difficult task to accomplish, especially in the present case where the structural distortions are sensitive to weak solid-state interactions. It appears that the angles θ_s and θ_2 are directly related with the equilibrium constants of compounds Pt(pqx)Cl_2 and Pt(pbqx)Cl_2, indicating that obtuse dihedral angles facilitate the dissociation of the chelates.

Conclusions

Based in ^{1}H NMR spectroscopic techniques it was showed that ligands pqx and pbqx in $CDCl_3$ solution prefer the *anti* configuration which stabilizes through two weak hydrogen bonds between H3'-N1 and H3'-N1. This configuration leads to the N4 monodentate coordination of pqx and pbqx in the complexes *trans*-Pt(DMSO)(pqx)Cl_2 (**2**) and *trans*- Pt(DMSO)(pbqx)Cl_2 (**4**) in low temperature (~15 °C). The *trans*- configuration of the complexes (**2**) and (**4**) may be explained assuming that the reaction mechanism passes through a five-coordinated intermediate, a rearrangement of the ligands followed by a withdrawal of a DMSO.

The crystal structures of the complexes (**1**), (**3**) and (**5**) showed a significant deviation of the planar geometry and high values of the distortion parameters θ_s and θ_2 reflecting the effect of the fused ring of the ligands pqx, pbqx, and pqn on the coordination geometry. This is most likely a reasonable factor for the solvolysis of the above complexes in DMSO-d_6, forming the complex *cis*-Pt(DMSO-d_6)$_2Cl_2$ and the free ligand. Instantaneous DMSO-d_6 solvolysis for the complexes (**1**) and (**3**) and slow kinetics solvolysis for (**5**) with rate constant $k = 10^{-4} \pm 6.4 \times 10^{-6}$ s^{-1}, reflect their differences in the distortion parameters. The titration of the complexes (**1**) and (**3**) with DMSO-d_6 revealed a two-step mechanism of the chelate ring opening, in fast ($k_1 > 10^5$ s^{-1}) and slow ($k_2 < 10^{-1}$ s^{-1}) kinetics in the NMR time scale at 298 K. In the first step of the reaction, the cleavage of one Pt-N bond was observed, which is more favorable for Pt-N1'. The equilibrium constants K_{eq} for the overall solvolysis reaction were calculated as $K_{eq} = 1.7 \times 10^{-4} \pm 0.2\times 10^{-4}$ for (**1**), and $K_{eq} = 4.1 \times 10^{-4} \pm 0.2$ M^{-1}, for (**2**).

These findings may be useful in the synthesis of platinum complexes, cytotoxic experiments, as well as in the design of platinum anticancer drugs, since ligands with high distortions may be utilized as good leaving groups under proper conditions.

View Article Online
DOI: 10.1039/C6DT04035G

Acknowledgments

We would like to thank Prof. A. J. Tasiopoulos at the University of Cyprus for facilitating of the X-ray difractometer. Also, we acknowledge the Unit of Environmental, Organic and Biochemical high resolution analysis-ORBITRAP-LC-MS and the NMR Center of the University of Ioannina for providing access to the facilities.

Supplementary Material

Figures of ^{1}H NMR titration with DMSO-d_6 of the complexes (**1**) and (**3**) and ^{1}H NMR spectra of (**5**) vs. time during its solvolysis in DMSO-d_6, are provided in the Supplementary Material in addition to the CIF files.

References

1. L. Kelland, *Nat. Rev. Cancer*, 2007, **7**, 573-584.

2. E. Wong, C.M. Giandomenico, *Chem. Rev.*, 1999, **99**, 2451–2466

3. S. Komeda, H. Takayama, T. Suzuki, A. Odani, T. Yamori, M. Chikuma, *Metallomics*, 2013, **5**, 461-468.

4. M. Uemura, T. Suzuki, K. Nishio, M. Chikuma, S. Komeda, *Metallomics*, 2012, **4**, 686-692.

5. Y. Yoshikawa, S. Komeda, M. Uemura, T. Kanbe, M. Chikuma, K. Yoshikawa, T. Imanaka, *Inorg. Chem.*, 2011, **50**, 11729-11735.

6. S. Komeda, *Metallomics,* 2011, **3**, 650-655.

7. S. Komeda, Y.-L. Lin, M. Chikuma, *ChemMedChem,* 2011, **6**, 987-990.

8. L. E. Wedlock, M. R. Kilburn, R. Liu, J. A. Shaw, S. J. Berners-Price, N. P. Farrell, *Chem. Commun.* 2013, **49**, 6944–6946

9. C. Manzotti, G. Pratesi, E. Menta, R. Di Domenico, E. Cavalletti, H. H. Fiebig, L. R. Kelland, N. Farrell, D. Polizzi, R. Supino, G. Pezzoni, F. Zunino, *Clin. Cancer Res.,* 2000, **6**, 2626–2634

10. B. J. Pages, Y. Zhang, F. Li, J. Sakoff, J. Gilbert, J. R. Aldrich-Wright, *Eur. J. Inorg. Chem.*, 2015, 4167-4175.

11. B. J. Pages, D. L. Ang, E. P. Wright, J. R. Aldrich-Wright, *Dalton Trans.*, 2015, **44**, 3505-3526.

12. B. W. J. Harper, J. R. Aldrich-Wright, *Dalton Trans.*, 2015, **44**, 87-96.

13. B.J. Pages, F. Li, P. Wormell, D.L. Ang, J. K. Clegg, C. J. Kepert, L. K. Spare, S. Danchaiwijit, J. R. Aldrich-Wright, *Dalton Trans.*, 2014, **43**, 15566-15575.

14. K. B. Garbutcheon-Singh, B. W. J. Harper, S. Myers, J. R. Aldrich-Wright, *Metallomics,* 2014, **6**, 126-131.

View Article Online
DOI: 10.1039/C6DT04035G

15. M. Cusumano, M. L. Di Petro, A. Gianneto, *Inorg. Chem.* 1999, **38**, 1754-1758,

16. M. Cusumano, M. L. Di Petro, A. Gianneto, P. A. Vainiglia, *J. Inorg. Biochem.,* 2005, **99**, 560-565.

17. M. D. Hall, K. A. Telma, K.-E. Chang, T. D. Lee, J. P. Madigan, J. R. Lloyd, I. S. Goldlust, J. D. Hoeschele, M. M. Gottesman, *Cancer Res.,* 2014, **74**, 3913-3922.

18. M. Calligaris, *Coord. Chem. Rev.*, 2004, **248**, 351-375.

19. (a) F. P. Fanizzi, F. P. Intini, L. Maresca, G. Natile, G. Uccello-Barretta, *Inorg. Chem.*, 1990, **29**, 29-33. (b) S. J. S. Kerrison, P. J. Sadler, *Inorg. Chim. Acta,* 1985, **104**, 197-201.

20. J. A. Platts, M. Ravera, E. Gabano, M. Sardi, S. Bianco, D. Osella, *Eur. J. Inorg. Chem.,* 2012, 5625-5631.

21. J. Yoo, J.-H. Kim, Y.S. Sohn, D. Youngkyu, *Inorg. Chim. Acta,* 1997, **263**, 53-60.

22. S. Kasselouri, A. Garoufis, A. Katehanakis, G. Kalkanis, S. P. Perlepes, N. Hadjiliadis, *Inorg. Chim. Acta,* 1993, 207, 255-258.

23. T. Tsolis, M. J. Manos, S. Karkabounas, I. Zelovitis, A. Garoufis, *J. Organomet. Chem,* 2014, **768**, 1-9.

24. C. M. Harris, S. Kokot, H. R. H. Patil, E. Sinn, H. Wong, *Aust. J. Chem.*, 1972, **25**, 1631-1643.

25. J. H. Price, A. N. Williamson, R. F. Schramm, B. B. Wayland, Inorg. Chem., 1972, **11**, 1280-1284.

26. M. Benedetti, F. De Castro, F. P. Fanizzi, Eur. J. Inorg. Chem. 2016, 3957–3962.

27. CrysAlis CCD and CrysAlis RED, Oxford Diffraction Ltd, Abingdon, Oxford, UK, 2009.

28. M. C. Burla, R. Caliandro, B. Carrozzini, G. L. Cascarano, C. Cuocci, C. Giacovazzo, M. Mallamo, A. Mazzone, G. Polidori, *J. Appl. Crystallogr.* 2015, **48**, 306-309.

29. G. M. Sheldrick, SHELXL 2014/7: Program for Crystal Structure Refinement, University of Göttingen, Germany, 2014.

30. A. L. Spek, PLATON: A Multipurpose Crystallographic Tool, Utrecht University, The Netherlands, 2008.

31. L. J. Farrugia, *J. Appl. Crystallogr.*, 1999, **32**, 837-838.

32. L. J. Barbour, *J. Supramol. Chem.* 2001, **1**, 189-191.

33. T. Pawlak, L. Pazderski, J. Sitkowski, L. Kozerski, E. Szłyk, *Magn. Reson. Chem.,* 2011, **49**, 59-64.

34. L. Pazderski, T. Pawlak, J. Sitkowski, L. Kozerski, E. Szłyk, *Magn. Reson. Chem.,* 2009, **47**, 932-941.

35. (a) F. D. Rochon, L. Fleurent, *Inorg. Chim. Acta,* 1988, **143**, 81-87. (b) J. R. L. Priqueler, I. S. Butler, F. D. Rochon, *Appl. Spectrosc. Rev.*, 2006, **41**, 185-226.

36. G. Annibale, M. Bonivento, L. Cattalini, M. L. Tobe, *J. Chem. Soc. Dalton Trans.,* 1992, 3433-3438.

View Article Online
DOI: 10.1039/C6DT04035G

37. F. Basolo, R. G. Pearson, *in Progress in Inorganic Chemistry* (F.A. Cotton ed.) vol. 4, Wiley Interscience, New York, 1962.

38. M. K. Cooper, J. M. Downes*, Chem. Commun.,* 1981, 381-382.

39. R. S. Bitzer, M. A. C. Nascimento, C. A. L. Filgueiras, *Polyhedron*, 2015, **102**, 329-336.

40. (a) C. A. Mitsopoulou, C. Dagas, *Bioinorg. Chem. Appl.*, 2010, no. 973742; (b) A. I. Philippopoulos, N. Tsantila, C. A. Demopoulos, C. P. Raptopoulou, V. Likodimos, P. Falaras, *Polyhedron*, 2009, **28**, 3310-3316; (c) W.-Y. Bi, W.-L. Chai, X.-Q. Lu, J.-R. Song, F. Bao, *J. Coord. Chem.*, 2009, **62**, 1928-1938; (d) C. A. Mitsopoulou, C. E. Dagas, C. Makedonas, *Inorg. Chim. Acta*, 2008, **361**, 1973-1982; (e) C. A. Mitsopoulou, C. E. Dagas, C. Makedonas, *J. Inorg. Biochem.,* 2008 **102**, 77-86; (f) S. I. Mostafa, (2007) *Trans. Met. Chem*., **32**, 769-775; (g) C. Makedonas, I. Veroni, C. A. Mitsopoulou, *Eur. J. Inorg. Chem.,* 2007, 120-131; (i) I. Veroni, C. Makedonas, A. Rontoyianni, C. A. Mitsopoulou, *J. Organomet. Chem.*, 2006, **691**, 267-281; (j) M. R. Waterland, S. L. Howell, K. C. Gordon, A. K. Burrell, *J. Phys. Chem.* A, 2005, **109**, , 8826-8833; (k) I. Veroni, A. Rontoyianni, C. A. Mitsopoulou, *Dalton Trans.,* 2003, 255-260; (l) C. Shao, W.-H. Sun, Z. Li, Y. Hu, L. Han, *Catal. Commun.,* 2002, **3**, 405-410; (m) S. I. Mostafa, S. P. Perlepes, N. Hadjiliadis, *Z. Naturforsch.* B, 2001, **56**, 394-402; (n) A. Garoufis, S. Kasselouri, C. P. Raptopoulou, *Inorg. Chem. Comm.,* 2000, **3**, 251-254; (o) S. Shanmuga Sundara Raj, H.-K. Fun, X.-F. Chen, X.-H. Zhu, X.-Z. You, Acta Cryst. C, 1999, **55** 2035-2037; (p) A. Garoufis, A. Koutsodimou, C. P. Raptopoulou, A. Simopoulos, N. Katsaros, *Polyhedron*, 1999, **18**, 3005-3012; (q) A. Garoufis, S. Kasselouri, S. Boyatzis, C. P. Raptopoulou, *Polyhedron*, 1999, **18**, 1615-1620; (r) A. Garoufis, A. Koutsodimou, N. Katsaros, C. A. Mitsopoulou, N. Hadjiliadis, *Polyhedron*, 1998, **18**, 361-369; (s) S. Kasselouri, A. Garoufis, S. P. Perlepes, F. Lutz, R. Bau, S. Gourbatsis, N. Hadjiliadis, *Polyhedron*, 1998, **17**, 1281-1288; (t) S. P. Perlepes, A. Garoufis, J. Sletten, E. G. Bakalbassis, J. Plakatouras, E. Katsarou, N. Hadjiliadis, *Inorg. Chim. Acta,* 1997, **261**, 93-102; (u) A. Garoufis, S. P. Perlepes, A. Schreiber, R. Bau, N. Hadjiliadis, *Polyhedron* 1996, **15**, 177-182; (v) S. P. Perlepes, S. Kasselouri, A. Garoufis, F. Lutz, R. Bau, N. Hadjiliadis *Polyhedron*, 1995, **14**, 1461-1470; (w) A. Garoufis, S. P. Perlepes, A. Vreugdenhil, I. S. Butler, N. Hadjiliadis, *Inorg. Chim. Acta*, 1995, **240**, 673-677.

41. A. Garoufis, S. P. Perlepes, N. A. Froystein, J. Sletten, N. Hadjiliadis, *Polyhedron,* 1996, **15**, 1035-1039.

42. S. Kasselouri, A. Garoufis, S. Paschalidou, S. P. Perlepes, I. S. Butler, N.Hadjiliadis, *Inorg. Chim. Acta,* 1994, **227**, 129-136.

43. V. Maheshwari, M. Carlone, F. R. Fronczek, L. G. Marzilli, *Acta Cryst.,* 2007, **B63**, 603-611.

44. V. M. Miskowski, V. H. Houlding, C.-M. Che, Y. Wang, *Inorg. Chem.*, 1993, **32**, 2518-2524

View Article Online
DOI: 10.1039/C6DT04035G

45. (a) C. Lopez, R. Bosque, M. Pujol, J. Simo, E. Sevilla, M. Font-Bardia, R. Messeguer, C. Calvis, *Inorganics*, 2014, **2**, 620-648; (b) F. Caruso, R. Spagna, L. Zambonelli, *Acta Cryst.,* 1980, **B36**, 713-715.

46. K. M. Anderson, A. G. Orpen, *Chem. Commun.,* 2001, 2682 – 2683.

47. W. B. Connick, L. M. Henling, R. E. Marsh, H. B. Gray, *Inorg. Chem.,* 1996, **35**, 6261-6265

48. A. J. Canty, M. G. Gardiner, R. C. Jones, M. Sharma, *Aust. J. Chem.*, 2011, **64**, 1355-1359

49. F. Basolo, R.G. Pearson, *Mechanism of Inorganic reactions*, Wiley, New York, 1967.

50. M. V. Twigg, *Mechanisms of Inorganic and Organometallic Reactions,* Plenum Press, New York, 1983

51. A. Hazell, *Polyhedron*, 2004, **23**, 2081-2083

52. (a) C. R. Groom, I. J. Bruno, M. P. Lightfoot, S. C. Ward, *Acta Cryst.*, 2016, **B72**, 171-179; (b) F. H. Allen, *Acta Cryst.,* 2002,**B58**, 380-388.

53. P. von Grebe, K. Suntharalingam, R. Vilar, P. J. S. Miguel, S. Herres-Pawlis, B. Lippert, *Chem. Eur. J.*, 2013, **19**, 11429-11438.

54. W. Kaim, A. Dogan, M. Wanner, A. Klein, I. Tiritiris, T. Schleid, D. J. Stufkens, T. L. Snoek, E. J. L. McInnes, J. Fiedler, S. Zalis, *Inorg. Chem.*, 2002, **41**, 4139-4148.

55. J. Bruce, D. Johnson, W. Cordes, R. Sadoski, *J. Chem. Cryst.*, 1997, **27**, 695-699

56. W. B. Connick, R. E. Marsh, W. P. Schaefer, H. B. Gray, *Inorg. Chem.*, 1997, **36**, 913-922

57. N. Okabe, Y. Muranishi, *Acta Cryst.,* 2005, **E61**, m2332-m2334

58. C. R. Barone, L. Maresca, G. Natile, C. Pacifico, *Inorg. Chim. Acta*, 2011, **366**, 384-387

59. F. P. Fanizzi, F. P. Intini, L. Maresca, G. Natile, M. Lanfranchi, A. Tiripicchio, *J. Chem. Soc., Dalton Trans.* 1991, 1007-1015

60. A. D. Bain, *Prog. Nuc. Magn. Reson Spectrosc.*, 2003, **43**, 63-103.

View Article Online
DOI: 10.1039/C6DT04035G

Chelated N-heterocycles can be replaced from the coordination sphere of square planar Pt(II) complexes by DMSO.